Cellular/Molecular

Independent Circadian Oscillations of *Period1* in Specific Brain Areas *In Vivo* and *In Vitro*

Ute Abraham,[1] Julie L. Prior,[2] Daniel Granados-Fuentes,[1] David R. Piwnica-Worms,[2] and Erik D. Herzog[1]

[1]Department of Biology, Washington University, St. Louis, Missouri 63130, and [2]Mallinckrodt Institute of Radiology, Molecular Imaging Center and Department of Molecular Biology and Pharmacology, Washington University School of Medicine, St. Louis, Missouri 63110

Behavioral and physiological circadian rhythms in mammals are controlled by a master pacemaker in the hypothalamic suprachiasmatic nuclei (SCN). Recently, circadian oscillations of hormone secretion, clock gene expression, and electrical activity have been demonstrated in explants of other brain regions. This suggests that some extra-SCN brain regions contain a functional, SCN-independent circadian clock, but *in vivo* evidence for intrinsic pacemaking is still lacking. We developed a novel method to image bioluminescence *in vivo* from the main olfactory bulbs (OB) of intact and SCN-lesioned (SCNX) *Period1::luciferase* rats for 2 d in constant darkness. The OBs expressed circadian rhythms *in situ* with a reliable twofold increase from day to night, similar to the phase and amplitude of *ex vivo* rhythms. *In vivo* cycling persisted for at least 1 month in the absence of the SCN. To assess indirectly *in vivo* rhythmicity of other brain areas, we measured the phase-dependence of their *in vitro* rhythms on the time of surgery. Surgery reliably reset the phase of the pineal gland and vascular organ of the lamina terminalis (VOLT) harvested from SCNX rats but had little effect on the phase of the OB. We deduce that the SCN and OB contain self-sustained circadian oscillators, whereas the pineal gland and VOLT are weak oscillators that require input from the SCN to show coordinated circadian rhythms. We conclude that the mammalian brain comprises a diverse set of SCN-dependent and SCN-independent circadian oscillators.

Key words: **suprachiasmatic nucleus; olfactory bulb; pineal gland; vascular organ of the lamina terminalis; bioluminescence; real-time imaging**

Introduction

Period1 (*Per1*) is a gene that is part of the transcriptional–translational feedback loop, which generates circadian rhythms in mammals and is rhythmically transcribed in the suprachiasmatic nuclei (SCNs) and many other tissues (Albrecht et al., 1997; Balsalobre et al., 1998; Yamazaki et al., 2000; Bae et al., 2001; Cermakian et al., 2001; Abe et al., 2002; Prolo et al., 2005). It remains controversial whether the daily rhythms in *Per1* expression in the body depend on the SCN. Although no residual behavioral, physiological, or molecular rhythms have been observed in SCN-lesioned (SCNX) animals maintained in prolonged constant conditions (Klein et al., 1991; Sakamoto et al., 1998; Meyer-Bernstein et al., 1999), a variety of tissues show rhythms *in vitro* (Tosini and Menaker, 1996; Abe et al., 2002; Granados-Fuentes et al., 2004b; Yoo et al., 2004). For example, circadian oscillations in *Per1* activity persist in the olfactory bulb (OB) when explanted from rats whose SCNs were arrhythmic or had been lesioned (Granados-Fuentes et al., 2004a). These rhythms are intrinsic to the mitral cell layer, entrainable, temperature compensated, correlated with firing rate patterns in individual OB neurons, and persist for at least 10 d *in vitro* (Granados-Fuentes et al., 2004b). Although the role of a circadian clock in any extra-SCN cell type is unclear, the OBs modulate photic responses in the SCN and show circadian differences in odor-induced immediate early gene expression (Amir et al., 1999a,b). Olfactory sensitivity may be modulated directly by peripheral circadian oscillators, as has been shown in the *Drosophila* antennas (Krishnan et al., 1999). Because no circadian oscillators have been shown to be SCN independent *in vivo*, we developed methods to record real-time gene activity *in situ*. We imaged bioluminescence from the bilateral OBs of intact and SCN-lesioned *Per1::luciferase* (*Per1::luc*) transgenic rats for 44–48 h. We found that the OBs contain an SCN-independent clock *in vivo* that expresses rhythms with a similar phase and amplitude *in vitro*.

Materials and Methods

Animals. Homozygous male transgenic *Per1::luc* rats (Japanese Wistar; gift from Dr. H. Tei, Mitsubishi Kagaku Institute for Life Sciences, Tokyo, Japan) expressing 6.7 kb of the mouse *Period1* promoter driving firefly luciferase (Yamazaki et al., 2000) were maintained in a 12 h light/dark cycle in the Hilltop Animal Facility at Washington University. Locomotor activity was recorded from rats housed individually in cages with continuous access to food, water, and a running wheel. Light level and wheel revolutions per minute were stored on a computer (Clocklab hardware and software; Actimetrics, Wilmette, IL). All procedures were in accordance with Institutional Animal Care and Use Committee and National Institutes of Health guidelines.

Received April 7, 2005; revised Aug. 9, 2005; accepted Aug. 9, 2005.

This work was supported by the National Institutes of Health (Grants MH63104 to E.D.H. and P50 CA94056 to D.R.P.-W.) and by the German Science Foundation (Grant AB139/3-1 to U.A.). We are grateful to Dr. Hajime Tei for the generous gift of the *Per1::luc* transgenic rats. We thank Laura Prolo, Erin Jackson, Lauren Krebs, and Fola Babatunde for their help with the OB *in vivo* imaging, Dr. Marty Straume for providing us with COSOPT, and Dr. Russ Van Gelder and an anonymous reviewer for helpful comments on a previous draft of this manuscript.

Correspondence should be addressed to Ute Abraham, Department of Biology, Washington University, Campus Box 1137, St. Louis, MO 63130. E-mail: Abraham@biology2.wustl.edu.

DOI:10.1523/JNEUROSCI.2225-05.2005

 0270-6474/05/258620-07$15.00/0

SCN lesion. SCN lesions were performed as described previously (Granados-Fuentes et al., 2004a). Wheel-running activity was recorded for up to 1 month after surgery, and arrhythmicity was confirmed using χ^2 periodogram analysis at the 0.01% confidence level (Clocklab; Actimetrics). Complete destruction of the SCN was verified postmortem by histological inspection. Sham lesions were performed identically with no current being passed.

In vivo *imaging.* Adult *Per1::luc* male rats were raised in the animal colony [lights on from 7:00 A.M. to 7:00 P.M. (LD); $n = 4$] or synchronized to a 12 h dark/light cycle for at least 2 weeks [lights on from 7:00 P.M. to 7:00 A.M. (DL); $n = 5$] or SCN lesioned, enucleated, and kept in constant darkness for 1 month ($n = 4$). When the rats were 48–65 d of age, 1–2 d before imaging, we prepared a glass window above the OB. Rats were anesthetized with 75 mg/kg ketamine hydrochloride (Ketaset; Fort Dodge Animal Health, Fort Dodge, IA), 0.5 mg/kg medetomidine hydrochloride (Domitor; Pfizer, Exton, PA), and 3 mg/kg baytril (Bayer, Shawnee Mission, KS) and enucleated. LD rats were enucleated in room light during the subjective day, and DL rats were enucleated under dim red light during the subjective night. We drilled a 0.25 cm^2 opening through the skull above the OB, made a 3 mm incision through the dura mater above each bulb, and filled the hole with 1.5% sterile agarose (Sigma, St. Louis, MO) in artificial CSF (ACSF). An injection port (1-cm-long polyvinylchloride tubing; inside diameter, 0.5 mm; outside diameter, 1.52 mm) and a cover glass (~0.5 cm^2) were placed on the agarose and fixed with dental cement (Teets "Cold Cure;" A-M Systems, Sequim, WA). Anesthesia was reversed with 1 mg/kg atipamezole hydrochloride (Antisedan; Pfizer), 0.05 mg/kg buprenorphine (Buprenex; Reckitt Benckiser Pharmaceuticals, Richmond, VA), and 3 ml of lactated Ringer's solution, and the rats recovered for 24–48 h. Rats received an additional injection of buprenorphine and baytril in the morning of the 2 imaging days. On the first day of imaging, each rat was anesthetized with isoflurane (3% vaporized in O_2) at 7:00 A.M. [LD rats, circadian time (CT) 0; DL rats, CT 12], injected with beetle D-luciferin (10 μl of 20 mM in ACSF; Promega, Madison, WI) through the sterile port, and allowed to awaken. CT 0 and CT 12 are defined as light onset and offset in the previous light cycle, respectively. After 4 h, the rats were reanesthetized with isoflurane and imaged for 1 min with an ultra-sensitive CCD camera using the In Vivo Imaging System (IVIS 100; field of view, 10; bin factor, 2; 1/f stop; open filter; Xenogen, Alameda, CA). Rats received another injection of luciferin, were returned to their cage, and awoke within 3 min after removal of the anesthetic. This procedure was repeated every 4 h for 44 h, during which time the rats showed no adverse effects of repeated 20 min anesthesia. Photon flux from the OB increased ~1000-fold after luciferin administration. To verify that the luciferin dose we used was saturating, we injected a rat with 10 μl of 10 mM luciferin and 10 min later imaged its OB. After imaging, we injected the rat with 10 μl of 50 mM luciferin and imaged again. Total bioluminescence from the OB did not increase over the next 30 min, indicating that the first dose of luciferin was saturating (data not shown).

We treated a second group of transgenic rats (LD, $n = 1$; SCNX, $n = 7$; 45–55 d of age) as described above except that we implanted a miniosmotic pump (model 2ML1; Alzet; Durect, Cupertino, CA) into the peritoneal cavity, left the dura mater intact, and did not insert an injection port. The pump was filled with beetle D-luciferin (30 mg/ml in 0.1 M PBS, pH 7.2; Xenogen) and released 10 μl/h. Pump-implanted rats were anesthetized for <10 min for each image collection. Mean photon flux from the OB was ~10 times higher than the background. As a control, one rat had its pump removed after 36 h of imaging. Bioluminescence dropped to background levels within 2.5 h (data not shown). After *in vivo* imaging, rats were anesthetized with CO_2, rapidly decapitated, and their brains removed for *in vitro* tissue culture as described previously (Abe et al., 2002). Intact rats were killed between CT 11 and CT 15.5 and SCNX rats between 7:00 A.M. and 11:00 A.M.

In vitro *tissue culture.* We cultured tissues from rats exposed to 4 d (DD4; $n = 9$) or 30 d (DD30; $n = 10$) of constant darkness, SCN lesioned for 1 week ($n = 4$) or 1 month ($n = 9$), or sham lesioned for 1 week (sham; $n = 4$) as described previously (Abe et al., 2002). Briefly, animals were anesthetized with CO_2 and decapitated at different times with respect to the previous light/dark cycle (DD4, SCNX, and sham) or their locomotor activity rhythm (DD30). Their brains and pineal glands (PIs) were removed quickly and collected in chilled HBSS, pH 7.2 (Sigma), supplemented with 0.01 M HEPES (Sigma), 100 U/ml penicillin, 0.1 mg/ml streptomycin, and 4 mM $NaHCO_3$ (Invitrogen, Carlsbad, CA). Coronal brain sections (300 μm) were obtained with a vibratome slicer (OTS-4000; Electron Microscopy Sciences, Fort Washington, PA), and the bilateral, medial SCN, unilateral, medial OB, and the medial part of the vascular organ of the lamina terminalis (VOLT) were dissected out using a pair of scalpels. The pieces of tissue or the whole pineal gland were cultured individually on a Millicell membrane (Millipore, Bedford, MA) in a Petri dish with 1 ml of DMEM (Sigma) supplemented with 10 mM HEPES (Sigma), 2.2 mg/ml $NaHCO_3$ (Invitrogen), and 0.1 mM beetle luciferin (Promega). Petri dishes were covered with glass slides, sealed with grease, and placed under photomultiplier tubes (HC135-11MOD; Hamamatsu, Shizouka, Japan) at 37°C in the dark. Bioluminescence was recorded in 1 min bins for at least 7 d.

Data analysis. Locomotor activity records were binned at 6 min intervals, and the last 10 d were analyzed for periodicity by χ^2 periodogram (Clocklab; Actimetrics). *In vivo* pseudocolor images obtained with the IVIS were analyzed using Living Image (Xenogen) and Igor (WaveMetrics, Portland, OR) software. Cosmic rays and background noise were automatically subtracted from the images. For each rat, total bioluminescence emitted from the area of the OB was measured as photons per second at each time point. Background was measured from the OB before luciferin administration for injected rats or from an area off the rat for implanted animals and subtracted from all OB measurements. Data were normalized to peak bioluminescence for each rat and averaged across all intact rats for each treatment at each circadian time. Data from individual rats were evaluated for rhythmicity by three independent methods: COSOPT (from Dr. Martin Straume, University of Virginia, Charlottesville, VA), daily crossings, and visual inspection. COSOPT has been used to detect circadian rhythms in 48 h data sets (Ceriani et al., 2002; Panda et al., 2002). Briefly, it calculates the least-squares optimized linear fit of 101 cosine functions to the detrended data. Subsequently, 1000 Monte Carlo randomizations are performed to assess the statistical probability of a significant rhythm being present (Straume, 2004). We report β as a measure of the rhythm amplitude (so that 2β approximates the peak-to-trough amplitude) and p as the probability that the measured rhythm arose randomly (significance level, $\alpha = 0.05$). The daily crossings method determined the number of cycles in the 48 h of imaging data. Original data were detrended by subtracting a 24 h running average. We measured the number of times the detrended data crossed a horizontal line through zero. Data sets that crossed this line fewer than three times or more than five times (e.g., more than three rising and two falling phases) were considered arrhythmic. Finally, three independent observers, blind to the experimental conditions, scored each bioluminescence trace as rhythmic or arrhythmic by visual inspection. When observer's opinions differed, the majority score was used. The three methods yielded identical results for 15 of the 21 records. COSOPT scored two records as rhythmic and one as arrhythmic, which were scored oppositely by the other methods. Visual inspection scored two more records as arrhythmic, which were scored as rhythmic by the other methods, and the daily crossings method scored one record as arrhythmic, which was scored as rhythmic by the other two techniques. Because the three methods produced similar estimates of rhythmicity (67% by visual inspection, 71% by daily crossings, and 81% by COSOPT), we used COSOPT to report the percentage rhythmic and period for all *in vivo* data. Average *in vivo* periods for intact and SCNX rats were calculated including only OB that were scored rhythmic by COSOPT.

The average *in vivo* bioluminescence was analyzed with COSOPT. To score rhythmicity conservatively, the significance level was calculated after a pseudo-Gaussian-distributed noise scaled to the SEM was added to the randomized data sets (to account for measurement errors). No multimeasures correction was applied (Straume, 2004).

In vitro bioluminescence recordings were detrended by subtracting a 24 h running average from the raw data. Subsequently, a 3 h running average was calculated from the detrended data. Crossover analysis (Abe et al., 2002) was then used to determine the time of peak bioluminescence. For the SCN, OB, and VOLT, the first peak of the recording was

selected, whereas for the PI, the second peak of the recording was used as a marker for the circadian phase *in vitro*. For intact rats, peak time was adjusted according to the period of each rat's locomotor activity rhythm. Only detrended bioluminescence traces that revealed a significant circadian period between 18 and 28 h as determined by fast Fourier transform–nonlinear least squares (Herzog et al., 1997) were included in the analysis (1 of 31 SCNs, 3 of 46 PIs, 1 of 41 VOLTs, and 3 of 45 OBs were excluded). Circadian peaks that reached at least 20% (10% for the PI) of the amplitude of the first circadian peak were used to determine the number of circadian cycles for each culture.

The times of peak expression of the OB *in vivo* and *in vitro* and times between surgery and peak phase of the other tissues *in vitro* were converted to degrees and tested for significant clustering of phases by the Rayleigh test (Batschelet, 1981). To correct for multiple testing, we set our significance level to 0.0125 for each test (Bonferroni's correction, 0.05 divided by the number of performed Rayleigh tests). *In vivo* and *in vitro* phases in *Per1::luc* of intact rats were tested for differences in their mean vectors using the Watson–Williams test (Batschelet, 1981). Results are presented as vector plots, and values are reported as mean vectors ± angular deviation (s). For the statistical analysis of the times between surgery and peak phase, data were assigned to 2 h intervals based on the time of surgery. When more than one rat was killed during a given interval, data were averaged. A maximum of 12 data points per tissue and condition were obtained and then analyzed using a Rayleigh test. To correct for multiple testing, we conservatively set our significance level to 0.0045 for each test (Bonferroni's correction, 0.05 divided by the number of performed Rayleigh tests).

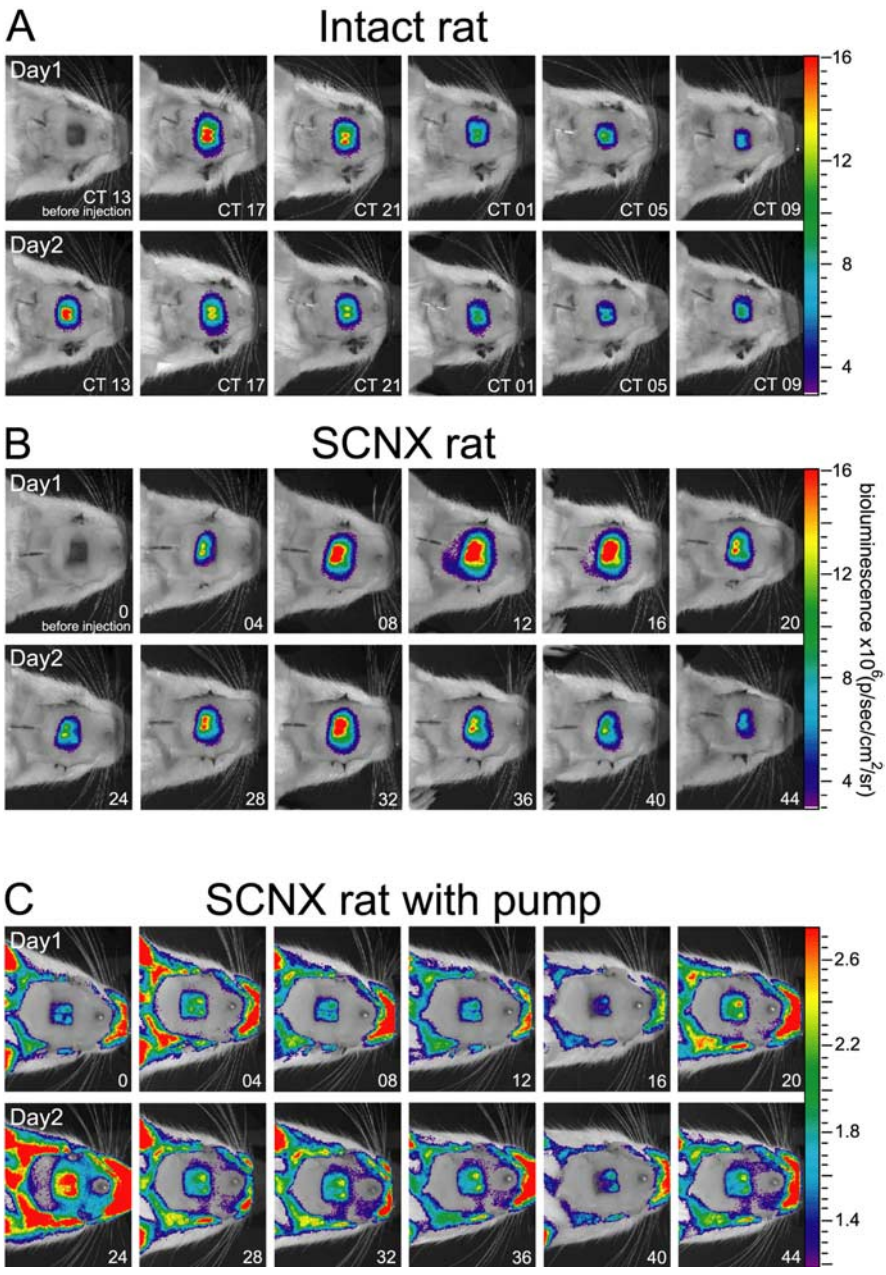

Figure 1. Representative *Per1::luc* bioluminescence images from the OB of three transgenic rats. Light from the bilateral OB was imaged for 1 min at 4 h intervals through a glass window in the skull in an intact (***A***) and SCNX (***B***) rat, 4 h after luciferin was delivered to the OB. Light emission peaked daily around CT 13–17 in the intact rat and around recording time 8–12 (3:00–6:00 P.M.) in the SCNX rat. Similarly, a circadian pattern of *Per1*-driven activity was seen in a SCNX rat carrying an osmotic pump releasing luciferin (30 mg/ml) at a rate of 10 μl/h (***C***). The pump was implanted in the intraperitoneal cavity 2 d before the start of imaging. Bioluminescence above background was emitted from the OB and exposed skin, although levels were ~10-fold lower than those from rats that received luciferin through a cannula. The intact rat was enucleated 2 d before the creation of the OB window, so all times are reported relative to the light/dark cycle to which the animal was entrained previously. CT 0 denotes the daily onset of the previous light phase (subjective dawn), and CT 12 denotes subjective dusk. For SCNX rats, which were enucleated and lesioned 1 month before the start of the imaging, recording started at 7:00 A.M. (time 0). Pseudocolored images were superimposed over a photograph of the anesthetized rats taken immediately before the bioluminescence integration.

Results

The OBs show rhythmic *Per1::luc* expression *in vivo*

After administration of luciferin *in vivo*, light emission from the OBs rapidly increased to ~1000-fold above background (Fig. 1*A*,*B*). Because of the local luciferin administration, bioluminescence was restricted to the OB and ranged from ~8×10^6 to 1×10^8 photons/s. In both the LD and DL groups, the OBs exhibited circadian oscillations in bioluminescence that peaked around early subjective night (CT 12–18). Circadian rhythms were detected in the *Per1*-activity patterns from three of four LD rats and four of five DL rats, as determined by COSOPT (Straume, 2004) (supplemental Fig. 1*A*,*E*, available at www.jneurosci.org as supplemental material).

In vivo imaging reveals OB rhythms that do not require the SCN

To test whether the OB continues to oscillate *in vivo* in the absence of the SCN, the OBs of SCNX rats that had been kept in constant darkness for 30 d were imaged in the same way as intact rats. All SCNX rats exhibited arrhythmic wheel-running activity in constant darkness (supplemental Fig. 1*B–D*, available at www.jneurosci.org as supplemental material) and complete destruction of the bilateral SCN on postmortem histological inspection. Two of the four SCNX rats displayed clear circadian rhythms of *Per1::luc* bioluminescence (Fig. 1*B*, supplemental Fig. 1F, available at www.jneurosci.org as supplemental material).

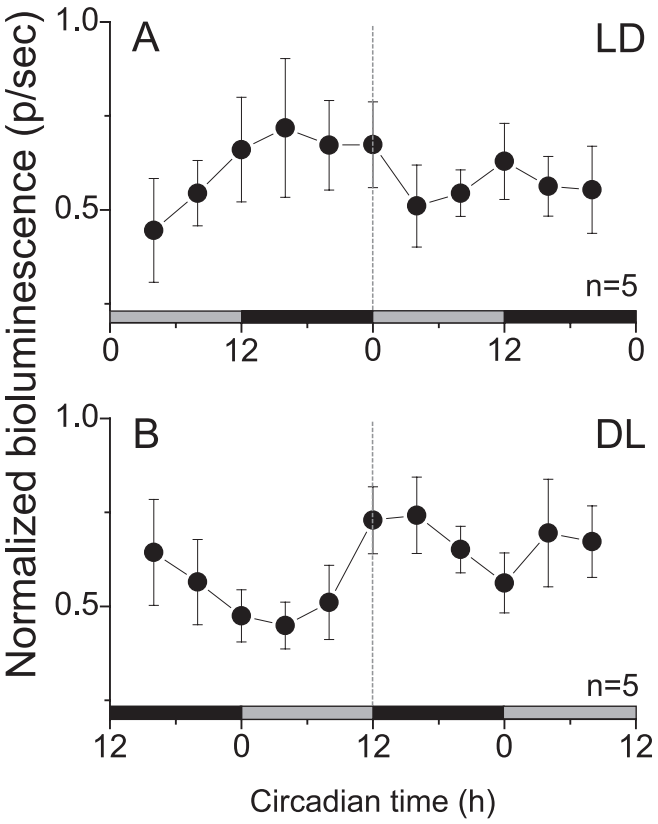

Figure 2. Average normalized photon flux emitted from the OB of intact rats was circadian over 2 d in constant darkness. Bioluminescence (mean ± SEM) of intact rats previously entrained to a LD cycle (***A***) or a DL cycle (***B***) peaked daily at about CT 15 in both groups. The peak-to-trough ratio for both groups averaged ~2:1. Gray and black bars denote the previous light and dark times, respectively. Values were normalized to the peak emission for each rat over the 48 h of imaging. Data from all OB (rhythmic and arrhythmic) were included in each condition.

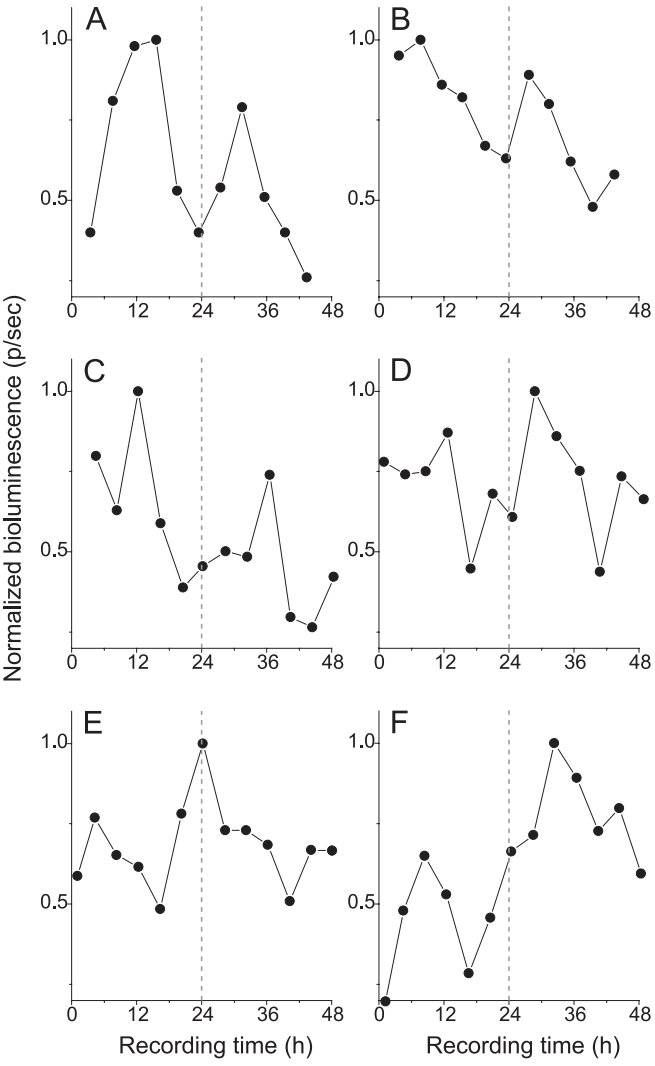

Figure 3. *In vivo* bioluminescence rhythms persist in the OBs of SCNX rats. Representative bioluminescence recordings from the *in vivo* OB of SCN-lesioned rats that received luciferin injections every 4 h (***A***, ***B***) or that were intraperitoneally implanted with luciferin-filled minosmotic pumps (***C–F***) are shown. All of these OB recordings were scored as rhythmic by COSOPT (***A***, $\beta = 0.27, p = 0.007$; ***C***, $\beta = 0.16, p = 0.033$; ***D***, $\beta = 0.14, p = 0.009$; ***E***, $\beta = 0.12, p = 0.01$; ***F***, $\beta = 0.18$, $p = 0.015$) with the exception of ***B***, which was scored as arrhythmic by COSOPT ($\beta = 0.12; p = 0.052$). Values were normalized to the peak emission for each rat over the 48 h of imaging.

We noted that the second peak of bioluminescence tended to be lower in amplitude in both intact and SCNX animals. To determine whether the prolonged anesthesia and repeated luciferin injections adversely affected rhythms in the OB, a separate group of LD ($n = 1$) and SCNX ($n = 7$) rats were implanted with an osmotic pump delivering luciferin into the peritoneal cavity at a constant rate. These animals were anesthetized for no >10 min every 4 h for the imaging, less than one-half the time experienced by luciferin-injected rats. We recorded bioluminescence from the OB ranging from 4×10^5 to 8×10^6 photons/s and from the exposed skin, particularly the ears and nose (Fig. 1*C*). All OBs in pump-implanted rats were rhythmic, which, when compared with 70% (9 of 13) rhythmic in luciferin-injected rats, indicates that the pump-implantation procedure yielded a higher success rate.

Combining the results of luciferin-injected and -implanted rats, we detected OB rhythms in 80% of the intact rats (8 of 10 rats in the LD and DL groups) and in 82% of the SCNX rats (9 of 11 rats). The average bioluminescence in LD and DL rats peaked in the early-to-mid subjective night (Fig. 2*A*,*B*), whereas individual SCNX rats peaked at various times after the start of the recording (see Fig. 3). All three groups showed rhythms with about a twofold increase in bioluminescence between peak and trough (COSOPT; DL; $\beta = 0.1$; $p = 0.045$) (Figs. 2, 3), although the LD oscillation did not reach statistical significance ($\beta = 0.1$; $p = 0.084$) unless random noise was omitted from the test ($\beta = 0.1$; $p = 0.009$). Thus, the amplitude of the *in vivo* OB rhythms is independent of the SCN and is similar to what has been reported for the OB *in vitro* (Granados-Fuentes et al., 2004a).

In vivo versus *in vitro* phasing of *Per1::luc* rhythms

To compare directly the rhythms recorded *in vivo* with those *in vitro*, we killed previously imaged rats and recorded bioluminescence from their OB *in vitro* (Fig. 4*A*,*B*). *In vivo*, the average period of the rhythmic OB in intact rats (23.1 ± 2.8 h SEM; $n = 8$) and SCNX rats did not significantly differ (22.3 ± 2.6 h; $n = 9$; Student's *t* test; $p > 0.05$) (Figs. 2, 3). *In vitro*, the OB of intact and SCNX rats also expressed similar average periods (intact rats, 22.8 ± 0.3 h, $n = 9$; SCNX rats, 21.9 ± 0.5 h, $n = 6$; Student's *t* test; $p > 0.05$). The *in vivo* phases of the OB from intact rats (CT 14.0 ± 1.7 h; $n = 7$; Rayleigh test; $r = 0.89$; $p < 0.001$) (Fig. 4*C*) were similar (Watson–Williams test; $F_{(2,14)} = 1.53$; $p > 0.05$) to those seen *in vitro* (CT 15.6 ± 2.6 h; $n = 9$; $r = 0.73$; $p = 0.004$),

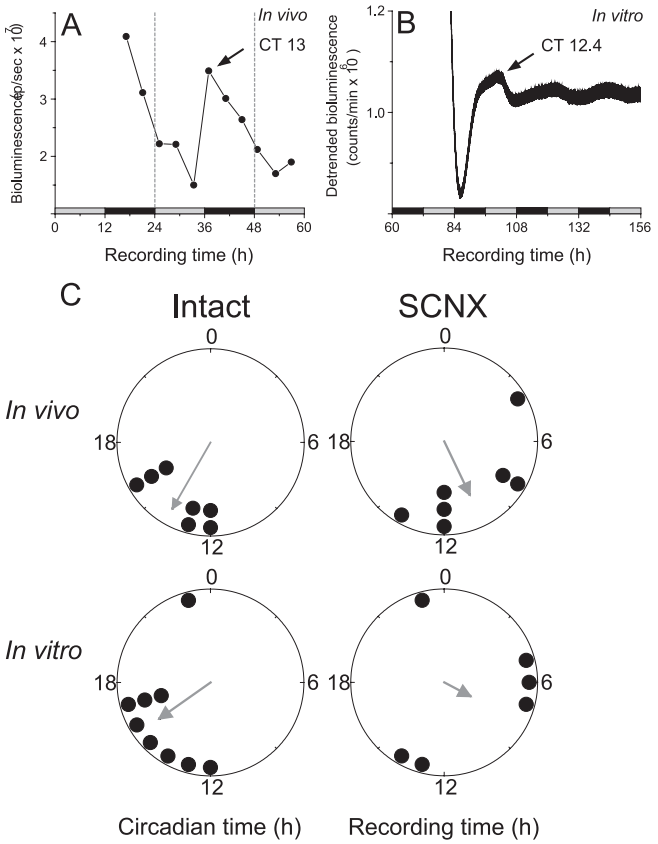

Figure 4. *Per1*-promoter activity was similar *in vivo* and *in vitro*. Representative bioluminescence recordings from the *in vivo* OB of the rat shown in Figure 1*A* (***A***) and the *in vitro* OB of a different rat (***B***). The recording time *in vivo* continues *in vitro* to illustrate that the OB were imaged for 44 h *in vivo* and then explanted for *in vitro* monitoring of bioluminescence. Light emission was circadian, peaking around CT 13 on the second day of *in vivo* imaging and then at CT 12.4 during the first 24 h *in vitro*. The free-running period of the OB was ~20–24 h *in vivo* and 22.2 ± 0.07 h *in vitro*. The times of previous light and dark are depicted by gray and black bars, respectively. ***C***, The *in vivo* (top row) and *in vitro* (bottom row) phases of peak *Per1::luc* expression were similar in the OB of intact rats (left). In contrast, the OB of SCNX rats (right) were more broadly distributed *in vivo*, peaking ~4 h earlier than those of intact rats, and were randomly distributed *in vitro*. The direction of the gray arrows denotes the mean phase of each condition and its length measures the tendency of the data to cluster based on a Rayleigh test where *r* values range from 0 (randomly phased) to 1 (all OB peaked at the same time).

whereas the OB of SCNX rats tended to peak at a different time (10.3 ± 3.0 h; $n = 7$; $r = 0.69$; $p = 0.025$) than the OB of intact rats *in vivo* (Watson–Williams test; $F_{(2,12)} = 5.97$; $p < 0.05$). These results indicate that the phases of OB rhythms from intact rats are similar *in vivo* and *in vitro*. Importantly, the phases of OB rhythms in SCNX rats were more broadly distributed and clustered at a time different from in intact rats, suggesting that the additional month in constant darkness allowed the phase of the OB to drift relative to the light cycle.

OB and SCN rhythms are less sensitive to the time of surgery than pineal and VOLT rhythms

Consistent with what has been reported previously (Granados-Fuentes et al., 2004a), the *in vitro* phases of the OB taken from SCNX rats killed between 7:00 A.M. and 11:00 A.M. were distributed randomly ($n = 6$; Rayleigh test; $r = 0.35$; $p = 0.52$) (Fig. 4*C*). This is, however, not consistent with the clustered phases seen *in vivo* and suggests that explanting these tissues from SCNX rats alters their timing. We reasoned that, if *in vitro* surgery induced *Per1* oscillations, the first peak of the subsequent rhythm would

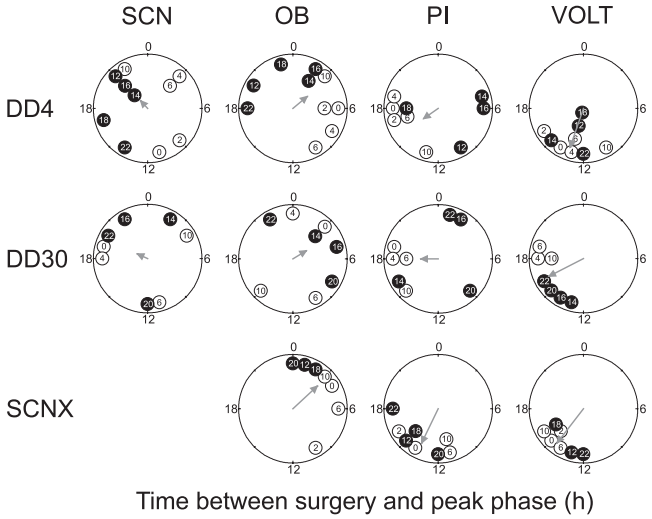

Figure 5. Polar plots showing the average times between the *in vitro* surgery (time 0) and the *Per1::luc in vitro* phase (circles). Tissues were derived from intact rats that had been in constant darkness for 4 d or 1 month or from rats that had been SCN lesioned for 1 month. The phases of animals that were killed within the same 2 h interval were averaged, and the surgery interval is given inside each circle (e.g., 14 = killed between CT 14 and CT 16). Open and filled circles represent surgery times during the subjective day and night, respectively. Gray arrows represent the mean vectors as in Figure 3. Surgery caused significant phase clustering of the PIs and VOLTs from SCNX rats and of the VOLTs from DD4 and DD30 rats (Rayleigh test; $\alpha = 0.0045$; Bonferroni's correction). In contrast, the phases of the SCNs and OBs were more broadly distributed, indicating that culturing did not reset their rhythmicity. Statistics were performed on averaged data to control for unequal sampling.

reliably follow the time of surgery. Therefore, we killed rats at different times during their circadian cycles, explanted the SCN, OB, PIs, and the VOLTs, and determined the time between surgery and the first peak in *Per1* activity. We found that the *in vitro* phases in the SCN were independent of the time of surgery when they were killed after 4 d in constant darkness (Rayleigh test; $n = 10$; $r = 0.22$; $p = 0.63$) (Fig. 5) or after 30 d in DD ($n = 8$; $r = 0.24$; $p = 0.65$; significance level was set to 0.0045 according to the Bonferroni's correction for multiple tests). This is in agreement with what is expected from a master circadian pacemaker in which oscillations are self-sustained and only modestly adjusted to perturbation.

Explants of the OB peaked at random times after the surgery on day 4 ($n = 10$; $r = 0.41$; $p = 0.205$) and day 30 in constant darkness ($n = 8$; $r = 0.34$; $p = 0.41$). Similarly, the phasing of the PI failed to show significant dependence on the time of surgery at DD4 ($n = 9$; $r = 0.39$; $p = 0.28$) or DD30 ($n = 8$; $r = 0.38$; $p = 0.33$). In contrast to the SCN, OB, and PI, the VOLT displayed a strong phase dependence on surgery time at DD4 ($n = 9$; $r = 0.90$; $p < 0.001$) and at DD30 ($n = 7$; $r = 0.85$; $p = 0.002$).

When explanted from SCNX rats, all brain areas tested showed circadian oscillations *in vitro* that were similar to those in sham-lesioned rats (supplemental Fig. 2, available at www.jneurosci.org as supplemental material). However, the PI ($n = 8$; $r = 0.83$; $p = 0.002$) (Fig. 4) and VOLT ($n = 7$; $r = 0.94$; $p < 0.001$) reliably peaked at ~14 h after explantation, whereas the OB were distributed randomly ($n = 7$; $r = 0.73$; $p = 0.015$). Thus, the phase of *in vitro* rhythms indicates that the PI and VOLT, but not the OB and SCN, are reset by surgery.

Discussion

Yamaguchi et al. (2001) showed that *Per1::luc* bioluminescence rhythms can be measured from the mouse SCN with a fiber optic.

Using a sensitive camera, we provide the first direct evidence of SCN-independent rhythms in the *in vivo* brain. We find that the OBs express similar daily rhythms in intact and SCNX rats, *in vivo* and *in vitro*. The approximately twofold changes in rhythm amplitude *in vivo* and *in vitro* are comparable with what has been reported for *in vivo Per1* and *Per1::luc* in the SCNs of rats and mice (Yamaguchi et al., 2001; Nagano et al., 2003; De la Iglesia et al., 2004). Because rats exposed to reversed light cycles showed rhythms that were oppositely phased, we exclude the possibility that surgery or repeated anesthesia induced the changes in bioluminescence. Furthermore, SCN explants of rats whose OBs had been imaged *in vivo* were all rhythmic and displayed similar circadian phases (11.6 ± 0.6 h SEM; $n = 11$) and periods (23.93 ± 0.12 h SEM; $n = 11$) to those of control rats (phase, 10.9 ± 0.9 h SEM, $n = 7$; period, 24.6 ± 0.3 h SEM, $n = 7$; Student's *t* test for phases, $p = 0.5$; for periods, $p = 0.07$), indicating that the surgical and imaging procedures did not interfere with the rats' health or circadian rhythms. We conclude that the OB express an entrained, circadian pattern of *Per1* gene activity *in vivo*. Photic entrainment likely requires the SCN, because the phase of OB rhythms depends on both the timing of the light cycle and the presence of a rhythmic SCN. Extensive, bidirectional, multisynaptic pathways between the SCN and OB may be involved (Shipley et al., 1985; Legoratti-Sanchez et al., 1989; Krout et al., 2002). Because *in vivo* OB rhythms persist for at least 30 d after SCN ablation and enucleation with circadian periods similar to *in vitro*, we conclude that OB cycling does not require the SCN or the eyes and is likely intrinsic to the OB.

What is the role then of the circadian clock in the OB? As in the *Drosophila* antennas, there may be local, circadian regulation of olfactory sensitivity (Krishnan et al., 1999; Tanoue et al., 2004; Zhou et al., 2005). Unlike sensory input to the visual, auditory, and somatosensory centers, information from the olfactory epithelium bypasses the thalamus (Butler and Hodos, 1996). Because a potential circadian gating mechanism, located in the thalamus and mediated by the SCN, is not available for the control of olfactory input, a circadian pacemaker in the OB could modulate daily olfactory function.

We were surprised to find that the OBs of SCNX rats tended to peak around the same time of day while the animals expressed no rhythms in locomotor activity. The similar phases may reflect similar free-running periods in their olfactory bulbs. This is supported by the fact that the OB of SCNX rats, which were imaged 1 month after enucleation and SCN ablation, were more broadly distributed and peaked on average at a different time than those of intact rats, which were imaged after 2 d in constant conditions. Alternatively, the surgery or repeated anesthesia could have induced or reset rhythms to a common phase in the OBs of SCNX rats. This is, however, unlikely because the time between creation of the OB window and the peak of the *in vivo* rhythm was uncorrelated (Rayleigh test; $n = 7$; $r = 0.44$; $p = 0.27$). Furthermore, the weak effects of surgery on the *in vitro* phasing of the OB support the conclusion that the OB are self-sustained circadian oscillators. Thus, the OB, like the SCN, appear to generate and coordinate circadian rhythms *in vivo*.

Our *in vivo* results are consistent with the conclusions of previous studies which inferred that some tissues including the OB do not require the SCN for sustained circadian rhythmicity (Granados-Fuentes et al., 2004a; Yoo et al., 2004). Our *in vitro* results, however, which show a tight phase relationship to the time of surgery for the PI and VOLT, indicate that the PI and VOLT are weaker circadian oscillators that likely require SCN input for sustained circadian oscillations *in vivo*. This is in agreement with numerous SCN ablation studies reporting the loss of rhythms, including those in melatonin secretion from the pineal gland (Meyer-Bernstein et al., 1999; Perreau-Lenz et al., 2003) or mRNA levels in the liver and other tissues (Sakamoto et al., 1998; Akhtar et al., 2002; Terazono et al., 2003; Amir et al., 2004; Guo et al., 2005). Given the recent observations that cultures of fibroblasts and zebrafish cell lines express damped circadian oscillations, whereas individual cells show sustained, but desynchronized, rhythms (Nagoshi et al., 2004; Welsh et al., 2004; Carr and Whitmore, 2005), we posit that individual pinealocytes and VOLT cells similarly lack the ability to synchronize their daily rhythms to each other and, therefore, result in damped rhythmicity on the tissue level. The VOLT might, thus, consist of cells with low-amplitude circadian oscillators that are easily reset by surgery. Pinealocytes from intact rats, which are less easily perturbed by surgery, may oscillate with higher amplitudes. Based on our *in vitro* data, we predict that *in vivo*, OB cells can synchronize their circadian rhythms to each other, whereas both the VOLT and PI lose coordinated circadian rhythmicity after SCNX, perhaps losing circadian synchrony and/or amplitude. Similar events may occur in the oval nucleus of the bed nucleus of the stria terminalis, which has been shown recently to require SCN input to sustain circadian rhythmicity *in vivo* (Amir et al., 2004). Thus, the SCN may play a critical role in synchronizing circadian oscillators in these tissues. We propose that the mammalian brain is organized around areas that generate rhythmicity autonomously and areas that require input to sustain or coordinate their daily oscillations.

References

Abe M, Herzog ED, Yamazaki S, Straume M, Tei H, Sakaki Y, Menaker M, Block GD (2002) Circadian rhythms in isolated brain regions. J Neurosci 22:350–356.

Akhtar RA, Reddy AB, Maywood ES, Clayton JD, King VM, Smith AG, Gant TW, Hastings MH, Kyriacou CP (2002) Circadian cycling of the mouse liver transcriptome, as revealed by cDNA microarray, is driven by the suprachiasmatic nucleus. Curr Biol 12:540–550.

Albrecht U, Sun ZS, Eichele G, Lee CC (1997) A differential response of two putative mammalian circadian regulators, mper1 and mper2, to light. Cell 91:1055–1064.

Amir S, Cain S, Sullivan J, Robinson B, Stewart J (1999a) In rats, odor-induced Fos in the olfactory pathways depends on the phase of the circadian clock. Neurosci Lett 272:175–178.

Amir S, Cain S, Sullivan J, Robinson B, Stewart J (1999b) Olfactory stimulation enhances light-induced phase shifts in free-running activity rhythms and Fos expression in the suprachiasmatic nucleus. Neuroscience 92:1165–1170.

Amir S, Lamont EW, Robinson B, Stewart J (2004) A circadian rhythm in the expression of PERIOD2 protein reveals a novel SCN-controlled oscillator in the oval nucleus of the bed nucleus of the stria terminalis. J Neurosci 24:781–790.

Bae K, Jin X, Maywood ES, Hastings MH, Reppert SM, Weaver DR (2001) Differential Functions of mPer1, mPer2, and mPer3 in the SCN circadian clock. Neuron 30:525–536.

Balsalobre A, Damiola F, Schibler U (1998) A serum shock induces circadian gene expression in mammalian tissue culture cells. Cell 93:929–937.

Batschelet E (1981) Circular statistics in biology. New York: Academic.

Butler AB, Hodos W (1996) Comparative vertebrate neuroanatomy. Evolution and adaptation. New York: Wiley.

Carr AJ, Whitmore D (2005) Imaging of single light-responsive clock cells reveals fluctuating free-running periods. Nat Cell Biol 7:319–321.

Ceriani MF, Hogenesch JB, Yanovsky M, Panda S, Straume M, Kay SA (2002) Genome-wide expression analysis in *Drosophila* reveals genes controlling circadian behavior. J Neurosci 22:9305–9319.

Cermakian N, Monaco L, Pando MP, Dierich A, Sassone-Corsi P (2001) Altered behavioral rhythms and clock gene expression in mice with a targeted mutation in the Period1 gene. EMBO J 20:3967–3974.

De la Iglesia HO, Cambras T, Schwartz WJ, Diez-Noguera A (2004) Forced

desynchronization of dual circadian oscillators within the rat suprachiasmatic nucleus. Curr Biol 14:796–800.

Granados-Fuentes D, Prolo LM, Abraham U, Herzog ED (2004a) The suprachiasmatic nucleus entrains, but does not sustain, circadian rhythmicity in the olfactory bulb. J Neurosci 24:615–619.

Granados-Fuentes D, Saxena MT, Prolo LM, Aton SJ, Herzog ED (2004b) Olfactory bulb neurons express functional, entrainable circadian rhythms. Eur J Neurosci 19:898–906.

Guo H, Brewer JM, Champhekar A, Harris RB, Bittman EL (2005) Differential control of peripheral circadian rhythms by suprachiasmatic-dependent neural signals. Proc Natl Acad Sci USA 102:3111–3116.

Herzog ED, Geusz ME, Khalsa SBS, Straume M, Block GD (1997) Circadian rhythms in mouse suprachiasmatic nucleus explants on multimicroelectrode plates. Brain Res 757:285–290.

Klein DC, Moore RY, Reppert SM (1991) Suprachiasmatic nucleus: the mind's clock. New York: Oxford UP.

Krishnan B, Dryer SE, Hardin PE (1999) Circadian rhythms in olfactory responses of *Drosophila melanogaster*. Nature 400:375–378.

Krout KE, Kawano J, Mettenleiter TC, Loewy AD (2002) CNS inputs to the suprachiasmatic nucleus of the rat. Neuroscience 110:73–92.

Legoratti-Sanchez MO, Guevara-Guzman R, Solano-Flores LP (1989) Electrophysiological evidences of a bidirectional communication between the locus coeruleus and the suprachiasmatic nucleus. Brain Res Bull 23:283–288.

Meyer-Bernstein EL, Jetton AE, Matsumoto SI, Markuns JF, Lehman MN, Bittman EL (1999) Effects of suprachiasmatic transplants on circadian rhythms of neuroendocrine function in golden hamsters. Endocrinology 140:207–218.

Nagano M, Adachi A, Nakahama K, Nakamura T, Tamada M, Meyer-Bernstein E, Sehgal A, Shigeyoshi Y (2003) An abrupt shift in the day/night cycle causes desynchrony in the mammalian circadian center. J Neurosci 23:6141–6151.

Nagoshi E, Saini C, Bauer C, Laroche T, Naef F, Schibler U (2004) Circadian gene expression in individual fibroblasts: cell-autonomous and self-sustained oscillators pass time to daughter cells. Cell 119:693–705.

Panda S, Antoch MP, Miller BH, Su AI, Schook AB, Straume M, Schultz PG, Kay SA, Takahashi JS, Hogenesch JB (2002) Coordinated transcription of key pathways in the mouse by the circadian clock. Cell 109:307–320.

Perreau-Lenz S, Kalsbeek A, Garidou ML, Wortel J, van der Vliet J, van Heijningen C, Simonneaux V, Pevet P, Buijs RM (2003) Suprachiasmatic control of melatonin synthesis in rats: inhibitory and stimulatory mechanisms. Eur J Neurosci 17:221–228.

Prolo LM, Takahashi JS, Herzog ED (2005) Circadian rhythm generation and entrainment in astrocytes. J Neurosci 25:404–408.

Sakamoto K, Nagase T, Fukui H, Horikawa K, Okada T, Tanaka H, Sato K, Miyake Y, Ohara O, Kako K, Ishida N (1998) Multitissue circadian expression of rat period homolog (rPer2) mRNA is governed by the mammalian circadian clock, the suprachiasmatic nucleus in the brain. J Biol Chem 273:27039–27042.

Shipley MT, Halloran FJ, de la TJ (1985) Surprisingly rich projection from locus coeruleus to the olfactory bulb in the rat. Brain Res 329:294–299.

Straume M (2004) DNA microarray time series analysis: automated statistical assessment of circadian rhythms in gene expression patterning. Methods Enzymol 383:149–166.

Tanoue S, Krishnan P, Krishnan B, Dryer SE, Hardin PE (2004) Circadian clocks in antennal neurons are necessary and sufficient for olfaction rhythms in *Drosophila*. Curr Biol 14:638–649.

Terazono H, Mutoh T, Yamaguchi S, Kobayashi M, Akiyama M, Udo R, Ohdo S, Okamura H, Shibata S (2003) Adrenergic regulation of clock gene expression in mouse liver. Proc Natl Acad Sci USA 100:6795–6800.

Tosini G, Menaker M (1996) Circadian rhythms in cultured mammalian retina. Science 272:419–421.

Welsh DK, Yoo SH, Liu AC, Takahashi JS, Kay SA (2004) Bioluminescence imaging of individual fibroblasts reveals persistent, independently phased circadian rhythms of clock gene expression. Curr Biol 14:2289–2295.

Yamaguchi S, Kobayashi M, Mitsui S, Ishida Y, van der Horst GT, Suzuki M, Shibata S, Okamura H (2001) View of a mouse clock gene ticking. Nature 409:684.

Yamazaki S, Numano R, Abe M, Hida A, Takahashi R, Ueda M, Block GD, Sakaki Y, Menaker M, Tei H (2000) Resetting central and peripheral circadian oscillators in transgenic rats. Science 288:682–685.

Yoo S-H, Yamazaki S, Lowrey PL, Shimomura K, Ko CH, Buhr ED, Siepka SM, Hong H-K, Oh WJ, Yoo OJ, Menaker M, Takahashi JS (2004) Period2::luciferase real-time reporting of circadian dynamics reveals persistent circadian oscillations in mouse peripheral tissues. Proc Natl Acad Sci USA 101:1–8.

Zhou X, Yuan C, Guo A (2005) *Drosophila* olfactory response rhythms require clock genes but not pigment dispersing factor or lateral neurons. J Biol Rhythms 20:237–244.